Theoretical Study on Adsorption of Na+ and Na+ (H2O)n (n = 1−6) on a Clean Si(111) Surface

3 AUTHORS, INCLUDING:

Yongjun Liu
Shandong University
87 PUBLICATIONS **514** CITATIONS

SEE PROFILE

Zhiguo Wang
Hangzhou Normal University
17 PUBLICATIONS **55** CITATIONS

SEE PROFILE

Theoretical Study on Adsorption of Na$^+$ and Na$^+$(H$_2$O)$_n$ (n = 1−6) on a Clean Si(111) Surface

Yongjun Liu,*,†,‡ Zhiguo Wang,† and Yourui Suo‡

School of Chemistry and Chemical Engineering, Shandong University, Jinan, Shandong, 250100, China, and Northwest Institute of Plateau Biology, Chinese Academy of Sciences, Xining,Qinghai, 810001, China

To model the adsorption of Na$^+$ in aqueous solution on the semiconductor surface, the interactions of Na$^+$ and Na$^+$(H$_2$O)$_n$ (n = 1−6) with a clean Si(111) surface were investigated by using hybrid density functional theory (B3LYP) and Møller−Plesset second-order perturbation (MP2) methods. The Si(111) surface was described with Si$_8$H$_{12}$, Si$_{16}$H$_{20}$, and Si$_{22}$H$_{21}$ cluster models. The effect of the basis set superposition error (BSSE) was taken into account by applying the counterpoise (CP) correction. The calculated results indicated that the interactions between the Na$^+$ cation and the dangling bonds of the Si(111) surface are primarily electrostatic with partial orbital interactions. The magnitude of the binding energies depends weakly on the adsorption sites and the size of the clusters. When water molecules are present, the interaction between the Na$^+$ and Si(111) surfaces weakens and the binding energy has the tendency to saturate. On a Si$_{22}$H$_{21}$ cluster described surface, the optimized Na$^+$−surface distance for Na$^+$(H$_2$O)$_5$ adsorbed at on-top site is 4.16 Å and the CP-corrected binding energy (MP2) is −35.4 kJ/mol, implying a weakly adsorption of hydrated Na$^+$ cation on clean Si(111) surface.

1. Introduction

Alkali metal atoms adsorption on semiconductor surface has received much attention for not only scientific interests but also for possible technological applications, such as in alkali metallization on ultrathin films, oxidation catalysis, and Schottky barrier formation.[1−16] As a model system, the Na/Si system has been intensively investigated by using numerous experimental and theoretical methods.[1−6,8−16] One might expect that the simple electronic configuration of Na (one valence electron) provides a clear-cut Na/Si interaction, i.e., the valence electron is completely transferred to the surface Si atom and an ionic bond is formed. Unfortunately, the real situation is far from being expected. The nature of Na/Si (dangling bonds) interaction has been controversial, showcased by the numbers of contradicting reports.[1−6,12,14] For example, from pseudopotential local density approximation calculations, Northrup[15] suggested that the alkali metals form strong ionic bonds on the Si(111) surface. Ossicini[2] investigated the electronic structure of the semiconductor−metal interface by using linear muffin-tin orbitals method in the atomic-sphere approximation and showed that a covalent character is dominant in the interaction. Clotet[5] used the ab initio Hartree−Fock cluster model approach to study the bond between alkali metals and Si(111) surface and found that the bond is highly ionic with a small covalent effect. Recently, Miyoshi[14] performed complete active-space self-consistent field (CASSCF) and multireference single and double excited configuration interaction calculations and concluded that the chemical bonds between Na and the Si(111) surface is essentially covalent. We believe that the contradicting results arise from usage of different models and methods. The structures and electronic properties of the interface should depend, in a great extent, on the adsorption site, surface coverage, and the type of silicon substrate.

Although electrodeposition, where ions in an aqueous solution are adsorbed on the surface to modify the properties of the semiconductor, is an important industrial process,[17] the study on the interaction between metal cation and semiconductor surface is still very limited. Numerous electrodeposition processes of metals on semiconductor surface are carried out in base electrolytes, therefore gaining the knowledge of the interaction between alkali metal cation and semiconductor surface is vital to understand the phenomena taking place at the solution/Si interface during the electrodeposition process. Recently, Pakkanen and co-workers[18] reported that the water molecules play different roles in the adsorption processes of Na$^+$ and Cu$^+$ cations onto the Cu(111) surface. To reveal the role water molecules play during the adsorption of alkali metal cations on to the semiconductor, we have investigated the hydrated Na$^+$/Si(111) and Na$^+$/Si(111) surfaces. The present work gives a first-principle investigation of the interaction between hydrated Na$^+$ and clean Si(111) surface and the role of water thereof.

2. Computational Methods

All the calculations were carried out by using the Gaussian 03 program package. The density functional theory (DFT) calculations using the hybrid Beck three-parameter with Lee−Yang−Parr correction functionals (B3LYP) and Møller−Plesset second-order perturbation method (MP2) were employed. The effective core potential LANL2DZ basis set was used for the Si atom, and the 6-31+G(d) basis set was used for the H, O, and Na atoms. In addition, the effect of the BSSE was compensated with the use of CP correction.

Miyoshi et al.[14] have used Si$_4$H$_7$ and Si$_7$H$_{10}$ cluster models to study the adsorption of Na and Mg atoms on a clean Si(111)

* To whom correspondence should be addressed. E-mail: yongjunliu_1@sdu.edu.cn. Fax: (+86) 531 885 644 64.
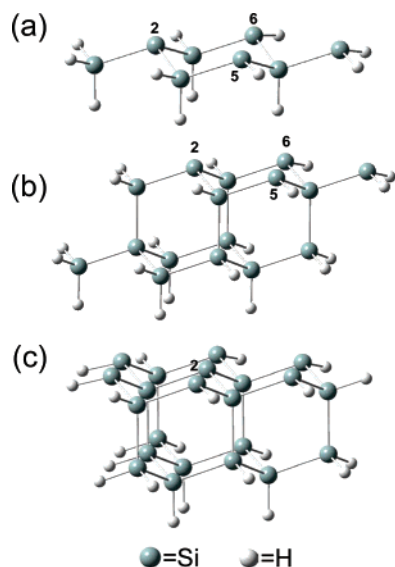† Shandong University.
‡ Chinese Academy of Sciences.

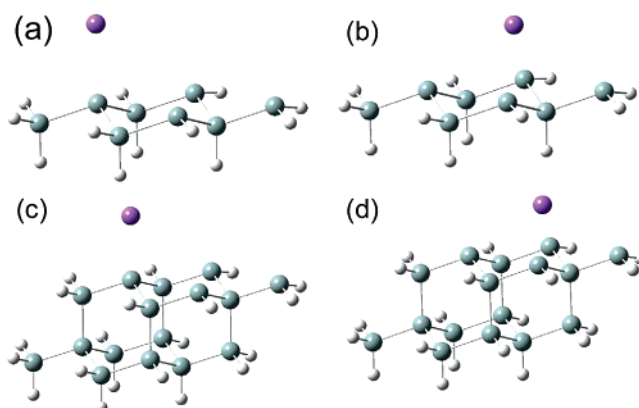**Figure 1.** Model clusters for clean Si(111) surface: (a) Si_8H_{12}; (b) $Si_{16}H_{20}$; (c) $Si_{22}H_{21}$.

Figure 2. Adsorption of Na atom and Na^+ on the surface of Si_8H_{12} and $Si_{16}H_{20}$. (a) and (c) are adsorbate (Na or Na^+) at the on-top (T) sites on the surfaces of Si_8H_{12} and $Si_{16}H_{20}$, respectively. (b) and (d) are adsorbate (Na or Na^+) at the bridge (T) sites, respectively.

surface. Clotet and co-workers[5] have used the $Si_{22}H_{21}$ cluster to investigate the nature of the chemisorption bond between an alkali metal, Li through Cs, and the Si(111) surface. We have taken a similar approach and used Si_8H_{12}, $Si_{16}H_{20}$, and $Si_{22}H_{21}$ clusters to model the interaction between the hydrated Na^+ cation and the Si(111) surface. Their structures are shown in Figure 1.

Si_8H_{12}, $Si_{16}H_{20}$, and $Si_{22}H_{21}$ clusters were cut from a bulk Si(111) surface. As shown in Figure 1, Si_8H_{12} is composed by a first and second layer, which contains four Si atoms in each layer. $Si_{16}H_{20}$ is constructed of four layers with four Si atoms in each layer. $Si_{22}H_{21}$ contains four layers with seven and three Si atoms in the first and fourth layers, and six Si atoms in the second and third layers. Each surface Si atom has an unpaired electron (dangling bond), and all the other bonds of the Si cluster were terminated with hydrogen atoms. The structures of Si_8H_{12}, $Si_{16}H_{20}$, and $Si_{22}H_{21}$ were optimized with all the positions of silicon atoms fixed.

It should be noted that the DFT and MP2 are useful only for the system dominated by a single electronic configuration. Therefore, we used CASSCF calculations to confirm that the clusters (Si_8H_{12} as the example) and their complexes with Na and Na^+ can be described by single electronic configuration.

3. Results and Discussions

3.1. Adsorption of Na and Na^+. Miyoshi et al.[14] have studied the adsorption of Na atom on the clean Si(111) surface and showed that the most favorable site is the on-top site. In this paper, for comparison, we examined the adsorption of Na atom and Na^+ cation at two adsorption sites: on-top (T) and bridge (B) sites, as shown in Figure 2. By adoption of Miyoshi and co-worker's procedure,[14] the adsorbate was allowed to move only perpendicular to the Si(111) surface while the geometry parameters of Si(111) moiety were fixed.

The geometries of Si_8H_{12}, $Na-Si_8H_{12}$, and $Na^+-Si_8H_{12}$ were optimized by using the CASSCF method, where all the dangling bonds of the surface Si atoms and 3s valence orbital of the Na atom were treated as active space. Therefore, there are four active electrons for Si_8H_{12} and $Na^+-Si_8H_{12}$ and five active electrons for $Na-Si_8H_{12}$. The calculated Na—Si distance of Na—Si_8H_{12} complexes at on-top (T) and bridge (B) sites are 2.79 and 2.45 Å, respectively, which is in an excellent agreement

with the reported values.[14] The coefficients of the dominant configuration of Si_8H_{12} and $Na^+-Si_8H_{12}$ are both larger than 0.9999; thus their electronic states can be described by single configurations. The coefficients of the dominant configuration of Na—Si_8H_{12} are 0.9999 and 0.9886 for on-top and bridge sites; therefore this can also be described approximately by single configuration.

The adsorption of Na and Na^+ on the surface of Si_8H_{12} and $Si_{16}H_{20}$ was studied by B3LYP and MP2 calculations. Because of the size of the clusters, the structures of all the complexes were first optimized with B3LYP and then energies were calculated by the MP2 method. The calculated structural parameters and binding energies are shown in Table 1.

The binding energies calculated by B3LYP and MP2 without BSSE correction are very similar except for the adsorption of Na atom on the bridge (B) site (Table 1). Because of the larger magnitude of BSSE calculated by MP2 compared to the value calculated by B3LYP method, there is a significant difference in the BSSE-corrected binding energies. There are some reports that CP results are overcorrection for MP2 calculations.[19,20] The validity of CP correction for MP calculations has been questioned because of its apparent utilization of perturbative correction related to excitations arising from ghost orbitals (orbitals which do not exist in the complex),[21] whereas study on water dimers showed that DFT (B3LYP) calculations provided the best CP-corrected energetic and geometric results.[22]

We also noted the great difference of adsorption between Na atom and Na^+. The binding energies of Na atom are much larger than that of Na^+ cation. The magnitude of the binding energies is nondependent to the size of the cluster for Na atom, where Na^+ showed dependency. On the other hand, the favorable adsorption site of Na atom is at the on-top (T) site while that of Na^+ is at the bridge (B) site. These results support the conclusion that nature of bonding between Na atom and the dangling bond is essentially covalent[14] while that of Na^+ cation are primarily electrostatic.

The Mulliken population analysis is listed in Table 2. The overlap population is a measure of the shared electronic density between two atoms, where large positive value indicates that the atoms in question are bonded and large negative value indicates that the atoms are in an antibond state. For the system of the on-top (T) site, the overlap populations of $Na-Si_2$ are as large as 0.254 and 0.223 in Na—Si_8H_{12} and Na—$Si_{16}H_{20}$, respectively. These values (0.254 and 0.223) are comparable to that of the normal Si—Si bonds in these clusters, displaying the characteristic of covalent bond. On the other hand, the

TABLE 1: Results for Na−Si$_8$H$_{12}$, Na$^+$−Si$_8$H$_{12}$, Na−Si$_{16}$H$_{20}$ and Na$^+$−Si$_{16}$H$_{20}$ by B3LYP and MP2 Calculations

	h_e (Å)^a	E_{tot} (au)^{b,c}	E_{tot}^{CP} (au)^{b,c}	E_b (kJ/mol)^e	E_b^{CP} (kJ/mol)^f	BSSE (kJ/mol)^g
			M−Si$_8$H$_{12}$ B3LYP			
Na−Si$_8$H$_{12}$ (T)	2.73	−200.34550	−200.34338	−172.5	−166.9	5.6
Na−Si$_8$H$_{12}$ (B)	2.31	−200.34352	−200.34090	−167.3	−160.4	6.9
Na$^+$−Si$_8$H$_{12}$ (T)	3.05	−200.10201	−200.10049	−54.8	−50.8	4.0
Na$^+$−Si$_8$H$_{12}$ (B)	2.51	−200.10896	−200.10676	−73.0	−67.3	5.8
			M−Si$_8$H$_{12}$ MP2			
Na−Si$_8$H$_{12}$(T)		−198.98535	−198.97556	−168.6	−142.9	25.7
Na-Si$_8$H$_{12}$ (B)		−198.97763	−198.96543	−148.4	−116.4	32.0
Na$^+$-Si$_8$H$_{12}$ (T)		−198.75950	−198.75250	−53.9	−35.5	18.4
Na$^+$-Si$_8$H$_{12}$ (B)		−198.76642	−198.75620	−72.1	−45.3	26.8
			M−Si$_{16}$H$_{20}$ B3LYP			
Na-Si$_{16}$H$_{20}$ (T)	2.73	−236.22691	−236.22487	−170.4	−165.1	5.4
Na-Si$_{16}$H$_{20}$ (B)	2.31	−236.22345	−236.22153	−161.3	−156.3	5.0
Na$^+$-Si$_{16}$H$_{20}$ (T)	2.97	−235.99377	−235.99222	−79.9	−75.9	4.0
Na$^+$-Si$_{16}$H$_{20}$ (B)	2.46	−236.00052	−235.99886	−97.6	−93.3	4.3
			M−Si$_{16}$H$_{20}$ MP2			
Na-Si$_{16}$H$_{20}$ (T)		−234.04204	−234.03158	−176.4	−148.9	27.5
Na-Si$_{16}$H$_{20}$ (B)		−234.03297	−234.02055	−152.5	−119.9	32.6
Na$^+$-Si$_{16}$H$_{20}$ (T)		−233.82307	−233.81486	−79.7	−58.2	21.5
Na$^+$-Si$_{16}$H$_{20}$ (B)		−233.82995	−233.81913	−97.8	−69.4	28.4

^{a} h_e denotes the equilibrium distance between the adsorbate and the Si(111) surface. ^{b} The total energies included zero-point-energy (ZPE) correction calculated by the B3LYP method. ^{c} MP2 energies calculated at B3LYP-optimized geometries. ^{d} CP-corrected energies. ^{e} $E_b = E_{tot} − (E_M + E_{Si(111)})$, where M = Na or Na$^+$. ^{f} CP-corrected values. ^{g} The difference between E_b and E_b^{cp}.

**TABLE 2: Mulliken Population Analysis of M−Si(111) by B3LYP Calculation**

	overlap population^a	
	on-top site	bridge site
Na−Si$_8$H$_{12}$	Na−Si$_2$: 0.254	Na−Si$_5$ (Si$_6$): 0.167
Na−Si$_{16}$H$_{20}$	Na−Si$_2$: 0.223	Na−Si$_5$ (Si$_6$): 0.168
Na$^+$−Si$_8$H$_{12}$	Na$^+$−Si$_2$: 0.108	Na$^+$−Si$_5$ (Si$_6$): 0.088
Na$^+$−Si$_{16}$H$_{20}$	Na$^+$−Si$_2$: 0.124	Na$^+$−Si$_5$ (Si$_6$): 0.095

^{a} The overlap population of the normal Si−Si bonds in Si$_8$H$_{12}$ and Si$_{16}$H$_{20}$ are 0.283 and 0.285, respectively.

overlap population of Na$^+$−Si$_2$ is only 0.108 for Na$^+$−Si$_8$H$_{12}$ and 0.124 for Na$^+$−Si$_{16}$H$_{20}$ (on-top site), which are much smaller than that of the normal Si−Si bonds (0.283 for Si$_8$H$_{12}$ and 0.285 for Si$_{16}$H$_{20}$). The relatively low values of overlap population of Na$^+$−Si$_8$H$_{12}$ and Na$^+$−Si$_{16}$H$_{20}$ indicate a non-bonded state between Na$^+$ and surface Si atom. To further explore the nature of bonding between Na$^+$ and Si(111) surface, the frontal orbital interactions in the complex of Na$^+$−Si$_8$H$_{12}$ (on top site) are examined (Figure 3). Figure 3 indicates that the s orbital of Na atom interacts with the p$_z$ orbital of the Si$_2$ atom resulting in the enlargement of energy gap between HOMO-2 and HOMO-3. The results suggest that interactions between Na$^+$ cation and the dangling bond of the Si(111) surface are primarily electrostatic with partial orbital interactions.

3.2. Adsorption of Na$^+$(H$_2$O)$_n$. Since the interactions between Na$^+$ cation and the dangling bonds of the Si(111) are primarily electrostatic, we first used the medium size cluster model, Si$_{16}$H$_{20}$, to investigate the adsorption of hydrated Na$^+$ cation on Si(111) surface. We have considered the adsorption on bridge (B) and on-top (T) sites.

The hydrated Na$^+$ cation, Na$^+$(H$_2$O)$_n$, complexes have been studied theoretically by Glendening and Feller,[23,24] Hashimoto and Morokuma,[25] and Baushlicher et al.[26] In this paper, the geometries of the Na$^+$(H$_2$O)$_n$ ($n = 1−6$) were fully optimized by the B3LYP/6-31+G(d) method and confirmed by vibrational analysis (Figure 4). For $n = 1−4$, water molecules are bound directly to the Na$^+$ ion by oxygen atoms avoiding the repulsion among the water molecules. The geometrical parameters are in excellent agreement with the results estimated by SCF and
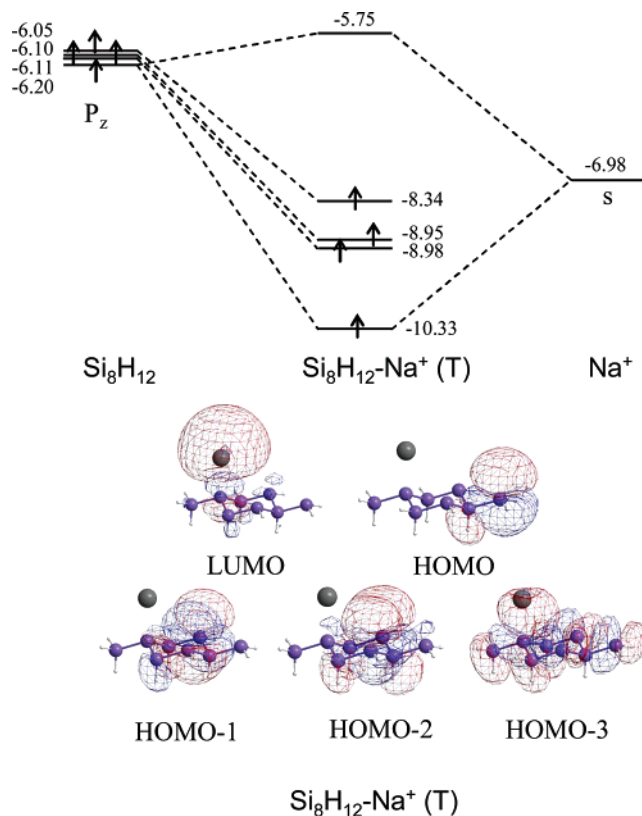
Figure 3. B3LYP/6-31+G(d) orbital interaction diagram of Si$_8$H$_{12}$−Na$^+$(T). Orbital energies are in eV.

MP2.[26] The successive H$_2$O binding energies of Na$^+$(H$_2$O)$_n$ correlate well with the experimental and theoretical works.[26,27] For the cation complexes with five or more water molecules, the most stable structure was found to be derived from the tetrahedral arrangement in Na$^+$(H$_2$O)$_4$ with more water molecules hydrating on the outside.[25] But in this paper, we have only studied the meta-stable structures that have the similar geometries with the cation complexes on the Si(111) surface. All the data are summarized in Table 3.
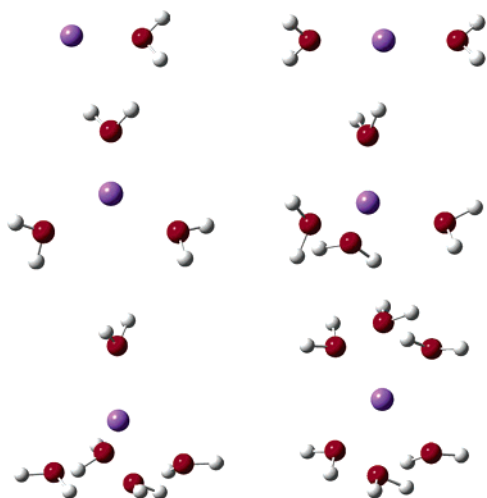
Figure 4. Optimized structures of $Na^+(H_2O)_n$ ($n = 1-6$) at the B3LYP/6-31+G(d) level.

Figure 5. Optimized structures of $Na^+(H_2O)_n$ ($n = 1-6$) adsorbed on the surface of $Si_{16}H_{20}$ cluster. (a) On-top site; (b) bridge site. The distance of Na^+−surface is in 0.1 nm.

To obtain the equilibrium geometries of the hydrated Na^+ cation on the clean Si(111) surface, as the first step, one to six water molecules were positioned around the Na^+ cation. Na^+ was allowed to move only perpendicular to the Si(111) surface, where no restrictions were placed to the water molecules. We found that the initial position(s) of the water molecules had no effect on the final structures since the optimization algorithm derives same optimal structure even with different initial geometries. The final adsorbate geometries are shown in Figure 5.

Figure 5 shows that the structures of the $Na^+(H_2O)_n$ ($n = 1-6$) on the Si(111) surface are different from the separately optimized structures. The relative position of the water molecules change a lot; however, the bond length of Na^+−O changes only slightly. It is due to the multiple interactions of water−water, water−Na^+, surface−water, and surface−Na^+. The interactions of water−water and water−Na^+ make the adsorbate to keep the structures as freely $Na^+(H_2O)_n$ complexes. On the other hand, the interactions of surface−water and surface−Na^+ constrain the positions of water molecules and Na^+ in order to maintain the optimal surface water and surface−Na^+ distances. We performed a B3LYP geometry optimization with the $Si_{22}H_{21}$ cluster with a single water molecule, where the optimal distance between the oxygen of water molecule and surface was estimated to be 2.73 Å.

The geometry optimization suggested that as the number of water molecules (n) increases, the Na^+−surface distance increase (see Figure 5). For the adsorption of the on-top (T) site, when n increases from 1 to 4, the distance of Na^+−surface (R_{eq}) changes smoothly from 3.02 to 3.68 Å. However, as n grows to 5, the value of R_{eq} increases sharply from 3.68 to 4.32 Å, which is in ac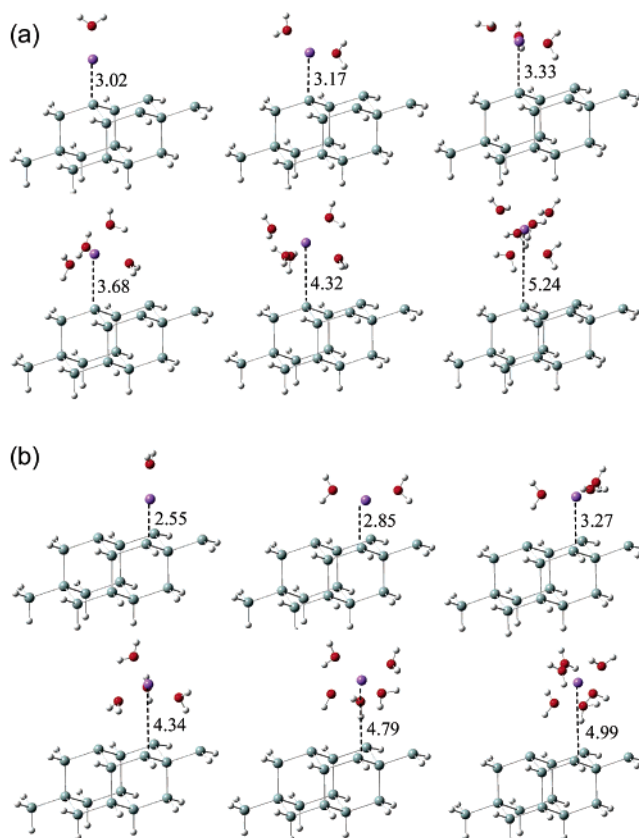cord with the sharp decrease of the binding energies (see Table 4). The adsorption of on bridge (B) site shows the similar case. When n increases from 1 to 3, the distance of Na^+−surface (R_{eq}) changes smoothly from 2.55 to 3.27 Å. As n grows to 4, the value of R_{eq} increases sharply from 3.27 to 4.34 Å. The increase of the Na^+−surface distance implies that the presence of water molecules weaken the interaction between Na^+ and Si(111) surface. The energies of the related species and the binding energies were listed in Table 4.

Because the binding energies E_b and E_b^{cp} in Table 4 were calculated by subtracting the energies of the $Si_{16}H_{20}$ cluster and the separately optimized $Na^+(H_2O)_n$ complex from the total energy of the $Si_{16}H_{20}-Na^+(H_2O)_n$ system, the binding energies include the (de)stabilization energy, which results from the changes in the optimal geometry of the separately optimized $Na^+(H_2O)_n$ complex when it is brought from infinite separation to the vicinity of the surface.

Table 4 shows that the B3LYP binding energies (E_b) for $n = 1-4$ without BSSE correction agree very well with the MP2

TABLE 3: Optimized Parameters and Successive Binding Energies (E_b) of $Na^+(H_2O)_n$ ($n = 1-6$)

	R_{Na-O} (Å)^a		$E_{complex}$ (au)^c		$E_{complex}$ ^{cp} (au)^e		E^b (kJ/mol)			
	B3LYP	MP2^b	B3LYP	MP2^d	B3LYP	MP2	B3LYP^f	MP2^f	SCF^b	exp^g
$Na^+(H_2O)_1$	2.212	2.212	−238.522 18	−237.887 06	−238.520 44	−237.883 77	−99.0	−101. 0	−97. 5	−97.9
$Na^+(H_2O)_2$	2.235	2.232	−314.958 94	−314.111 60	−314.954 42	−314.103 14	−80.8	−87.6	−86. 2	−80.3
$Na^+(H_2O)_3$	2.260	2.251	−391.389 13	−390.329 43	−391.381 86	−390.317 04	−68.2	−73.3	−69. 5	−63.6
$Na^+(H_2O)_4$	2.289	2.276	−467.813 90	−466.542 82	−467.803 05	−466.525 05	−51.8	−56.5	−58. 2	−55.2
$Na^+(H_2O)_5$	2.274 (2.425)		−544.229 27	−542.749 67	−544.220 96	−542.733 73	−43.1	−52.5		−49.0
$Na^+(H_2O)_6$	2.430		−620.646 71	−618.958 26	−620.636 90	−618.939 47	−38.0	−44.8		−42.3

^{a} R_{Na-O} denotes the equilibrium distance between the Na^+ and oxygen atom in complexes. ^{b} Reference 26. ^{c} The total energies of $Na^+(H_2O)_n$ included zero-point-energy (ZPE) correction calculated by the B3LYP method. ^{d} MP2 energies calculated at B3LYP-optimized geometries. ^{e} CP-corrected energies. ^{f} $E_b = E_{Na^+(H_2O)_n}^{cp} - (E_{Na^+(H_2O)^{n-1}}^{cp} + E_{H_2O})$. ^{g} Reference 27.

TABLE 4: Results for Na⁺(H₂O)ₙ (n = 1−6) Binding on Si₁₆H₂₀ at T and B Sites

		E_{tot} (au)[a]		E_{tot}^{cp} (au)[b]		E_b (kJ/mol)[c]		E_b^{cp} (kJ/mol)[d]		BSSE (kJ/mol)[e]	
		B3LYP	MP2	B3LYP	MP2	B3LYP	MP2	B3LYP	MP2	B3LYP	MP2
T site	Si₁₆H₂₀−Na⁺(H₂O)₁	−312.42473	−310.04397	−312.42617	−310.03527	−60.8	-61. 7	-62.1	−47. 5	−1.3	14.2
	Si₁₆H₂₀−Na⁺(H₂O)₂	−388.85741	−386.26144	−388.85585	−386.25187	−43.0	−43. 1	−50.8	−40. 2	−7.8	2.9
	Si₁₆H₂₀−Na⁺(H₂O)₃	−465.28109	−462.47360	−465.27929	−462.46378	−25.9	−28. 2	−40.3	−35. 0	−14.4	−6.8
	Si₁₆H₂₀−Na⁺(H₂O)₄	−541.70038	−538.68094	−541.69768	−538.67076	−11.5	−12. 3	−32.9	−32. 3	−21.4	−20. 0
	Si₁₆H₂₀−Na⁺(H₂O)₅	−618.11529	−614.88397	−618.11262	−614.87462	−10.3	−2.3	−32.1	−19. 6	−21.8	−17. 3
	Si₁₆H₂₀−Na⁺(H₂O)₆	−694.53062	−691.09694	−694.52979	−691.08011	−4.8	12.4	−28.4	−19. 0	−23.6	−31. 4
B site	Si₁₆H₂₀−Na⁺(H₂O)₁	−312.43216	−310.04921	−312.43038	−310.03813	−73.2	−75. 4	−73.1	−54. 9	0.1	20.5
	Si₁₆H₂₀−Na⁺(H₂O)₂	−388.86028	−386.26432	−388.85811	−386.25328	−50.6	−50. 7	−56.9	−41. 5	−6.3	9.2
	Si₁₆H₂₀−Na⁺(H₂O)₃	−465.28155	−462.47359	−465.27901	−462.46377	−27.1	−28. 2	−39.6	−34. 9	−12.5	−6.7
	Si₁₆H₂₀−Na⁺(H₂O)₄	−541.70228	−538.67947	−541.70040	−538.67133	−16.5	−8.5	−40.0	−31. 4	−23.5	−22. 9
	Si₁₆H₂₀−Na⁺(H₂O)₅	−618.11735	−614.88319	−618.11616	−614.87384	−15.7	−0.3	−34.4	−20. 8	−18.7	−20. 5
	Si₁₆H₂₀−Na⁺(H₂O)₆	−694.53221	−691.08949	−694.53145	−691.08122	−9.0	5.7	−32.8	−22. 1	−23.8	−27. 6

[a] The total energies included zero-point-energy (ZPE) correction calculated by B3LYP method. MP2 energies calculated at B3LYP optimized geometries. [b] CP-corrected energies. [c] $E_b = E_{tot} − (E_{complex} + E_{Si(111)})$. [d] $E_b^{cp} = E_{tot}^{cp} − (E_{complex}^{cp} + E_{Si(111)}^{cp})$. [e] The difference between E_b and E_b^{cp}.
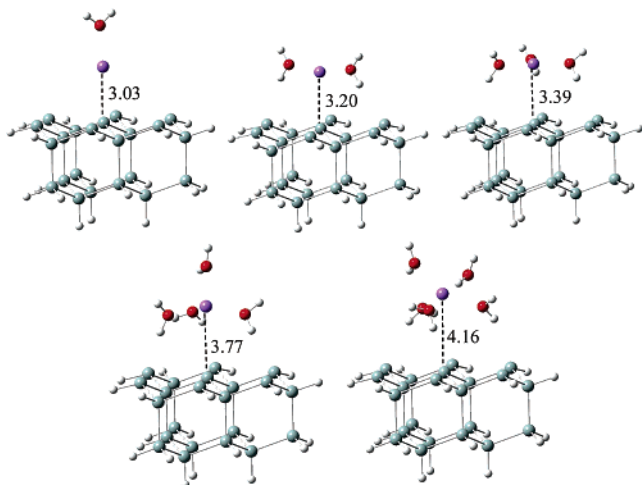

Figure 6. Optimized structures of Na⁺(H₂O)ₙ (n = 1−5) adsorbed on the surface of Si₂₂H₂₁ cluster at the on-top site. The distance of Na⁺−surface is in 0.1 nm.

results. But for n = 5−6, there is a difference between B3LYP and MP2 results. It is due to the large distance of Na⁺−surface and weak interaction of Na⁺(H₂O)ₙ and the surface. In this case, the electron-correlated theoretical method is needed.

Table 4 also shows that the value of BSSE changes greatly with the number of water molecules. This is because the total BSSE corrections were obtained by subtracting the BSSE correction of the separately optimized Na⁺(H₂O)ₙ complex from that of the Si₁₆H₂₀−Na⁺(H₂O)ₙ system. As the number of water molecules increases from 1 to 6, the BSSE correction of Na⁺(H₂O)ₙ complex increases from 4.6 to 25.8 kJ/mol (B3LYP method) and from 8.6 to 49.3 kJ/mol (MP2 method). On the other hand, the BSSE correction of Si₁₆H₂₀−Na⁺(H₂O)ₙ remains almost constant even as the number of water molecules changes. Therefore, the corresponding value of total BSSE corrections changes greatly with the number of water molecules.

To investigate the effect of the cluster size on the adsorption hydrated Na⁺ on clean Si(111) surfaces, we used the larger cluster model, Si₂₂H₂₁, to describe the Si(111) surface. The optimized structures of Na⁺(H₂O)ₙ (n = 1−5) adsorbed on the surface of Si₂₂H₂₁ cluster at on-top site are shown in Figure 6. The binding energies are listed in Table 5.

Figure 6 shows that the adsorbed Na⁺(H₂O)ₙ (n = 1−5) on the surface of the Si₂₂H₂₁ cluster have the similar geometries as those on Si₁₆H₂₀ cluster. In particular, they have the very similar Na⁺−surface distances. It implies that the interaction between Na⁺ and the dangling bond of the surface Si atom plays an important role in the adsorption of Na⁺(H₂O)ₙ on the Si-(100) surface. We also noted that the relative position of the water molecules changes slightly, which means the interaction between the water molecules and Si(111) surface changes with the number of surface Si atoms. An evidence is the increase of the binding energies on the larger cluster model (see Table 4). The B3LYP and MP2 calculated binding energies on Si₂₂H₂₁ cluster are about one-third percent larger than that on Si₁₆H₂₀ cluster. Although the magnitude of the binding energies is different, both models show the same tendency that binding energies (E_b^{cp}) become to saturate as the number of water molecules increases.

4. Conclusions

The adsorption of Na⁺ and hydrated Na⁺ on clean Si(111) surfaces were studied using hybrid DFT (B3LYP) and MP2 methods. The calculated results reveal that the interaction between Na⁺ cation and the dangling bond of the silicon surface is primarily electrostatic with partial orbital interactions. The magnitude of the binding energies between Na⁺ and the dangling bond depends on the adsorption sites and the size of the clusters. When water molecules are present, the interaction between Na⁺ and Si(111) surface weakens and the binding energy has the tendency to saturate as the number of water molecules increase. On a Si₂₂H₂₁ cluster described surface, the optimized Na⁺−

TABLE 5: Results for Na⁺ and Na⁺(H₂O)ₙ Binding on Si₂₂H₂₁ (n = 1−5) at T Site

	E_{tot} (au)[a]		E_{tot}^{cp} (au)[b]		E_b (kJ/mol)[c]		E_b^{cp} (kJ/mol)[d]		BSSE (kJ/mol)[e]	
	B3LYP	MP2	B3LYP	MP2	B3LY P	MP 2	B3LYP	MP2	B3LYP	MP 2
Si₂₂H₂₁−Na⁺	−259.85178	−257.16680	−259.84997	−257.84026	−87.8	−92. 0	−83.0	−66.5	4.8	25.5
Si₂₂H₂₁−Na⁺(H₂O)₁	−336.28506	−333.38770	−336.28380	−333.37901	−67.7	−73. 9	−67.5	−54.7	0.2	19.2
Si₂₂H₂₁−Na⁺(H₂O)₂	−412.71604	−409.60672	−412.71357	−409.59394	−52.5	−59. 4	−57.9	−48.1	−5.4	11.3
Si₂₂H₂₁−Na⁺(H₂O)₃	−489.14071	−485.81962	−489.13776	−485.80524	−38.0	−46. 4	−49.3	−41.2	−11.3	5.2
Si₂₂H₂₁−Na⁺(H₂O)₄	−565.56016	−562.02728	−565.55756	−562.01259	−24.1	−31. 4	−45.7	−39.5	−21.6	−8.1
Si₂₂H₂₁−Na⁺(H₂O)₅	−641.97474	−638.23142	−641.97223	−638.21684	−22.0	−24. 3	−41.2	−35.4	−19.2	−11. 1

[a] The total energies included zero-point-energy (ZPE) correction calculated by B3LYP method. MP2 energies were calculated at B3LYP optimized geometries. [b] CP-corrected energies. [c] $E_b = E_{tot} − (E_{complex} + E_{Si(111)})$. [d] $E_b^{cp} = E_{tot}^{cp} − (E_{complex}^{cp} + E_{Si(111)}^{cp})$. [e] The difference between E_b and E_b^{cp}.

Liu et al.

surface distance for $Na^+(H_2O)_5$ adsorbed at the on-top site is 4.16 Å and the CP-corrected binding energy (MP2 result) is -35.4 kJ/mol, implying a weakly adsorption of hydrated Na+ cation on clean Si(111) surface.

References and Notes

(1) Reihl, B.; Sorensen, S. L.; Dudde, R.; Magnusson, K. O. *Phys. Rev. B* **1992**, *46*, 1838.

(2) Ossicini, S.; Arcangeli, C.; Bisi, O. *Phys. Rev. B* **1990**, *42*, 7671.

(3) Jeon, D.; Hashizume, T.; Sakurai, T.; Willis, R. F. *Phys. Rev. Lett.* **1992**, *69*, 1419.

(4) Clotet, A.; Ricart, J. M.; Rubio, J.; Illas, F.; SanFadian, E.; Moscardo, F. *Phys. Rev. B* **1995**, *52*, 11998.

(5) Clotet, A.; Ricart, J. M.; Rubio, J.; Illas, F. *Phys. Rev. B* **1995**, *51*, 1581.

(6) Moullet, I.; Andreoni, W.; Parrinello, M. *Phys. Rev. B* **1992**, *46*, 1842.

(7) Grupp, C.; Taleb-Ibrahimi, A. *Surf. Sci.* **1998**, *408*, 160.

(8) Weitering, H. H.; Chen, J.; Pérez-Sandoz, R.; DiNardo, N. J. *Surf. Sci.* **1994**, *978*, 307−309.

(9) Jeon, D.; Hashizume, T.; Wang, X.; Motai, K.; Sakarai, T. *Appl. Surf. Sci.* **1993**, *67*, 257.

(10) Boness, J.; Marowsky, G.; Braun, J.; Witte, G.; Rubahn, H.-G. *Surf. Sci.* **1998**, *513*, 402−404.

(11) Hansen, P.-E.; Pedersen, K.; Liu, L.; Morgen, P. *Surf. Sci.* **1997**, *391*, 252.

(12) Clotet, A.; Ricart, J. M.; Rubio, J.; Illas, F. *Surf. Sci.* **1996**, *364*, 89.

(13) D'angelo, M.; Konishi, M.; Matsuda, I.; Liu, C.; Hasegawa, S.; Okuda, T.; Kinoshita, T. *Surf. Sci.* **2005**, *590*, 162.

(14) Miyoshi, E.; Mori, H.; Tanaka, S.; Sakai, Y. *Surf. Sci.* **2002**, *514*, 383.

(15) Northrup, J. E. *J. Vac. Sci. Technol. A* **1986**, *4*, 1404.

(16) Kravetsky, I. V.; Marowsky, G.; Rubahn, H.-G. *Surf. Sci.* **2001**, *474*, 47.

(17) Bunshah, R. F. In *Handbook of Deposition Technologies for Films and Coatings*, 2nd ed.; Noyes Publications: Park Ridge, NJ, 1994; p 23

(18) Karttunen, A. J.; Rowley, R. L.; Pakkanen, T. A. *J. Phys. Chem. B* **2005**, *109*, 23983.

(19) Rayon, V. M.; Sordo, J. A. *J. Phys. Chem. A* **1997**, *101*, 7414.

(20) Kim, K.; Jordan, K. D. *J. Phys. Chem.* **1994**, *98*, 10089.

(21) Cook, D. B.; Sordo, J. A.; Sordo, T. L. *Int. J. Quantum Chem.* **1993**, *48*, 375.

(22) Simon, S.; Duran, M.; Dannenberg, J. J. *J. Phys. Chem. A* **1999**, *103*, 1640.

(23) Glendening, E. D.; Feller, D. *J. Phys. Chem.* **1995**, *99*, 3060.

(24) Feller, D.; Glendening, E. D.; Woon, D. E.; Feyereisen, M. W. *J. Chem. Phys.* **1995**, *103*, 3526.

(25) Hashimoto, K.; Morokuma, K. *J. Am. Chem. Soc.* **1994**, *116*, 11436.

(26) Bauschlicher, C. W., Jr.; Langhoff, S. R.; Partridge, H. *J. Chem. Phys.* **1991**, *95*, 5142.

(27) Dzidic, I.; Kebarle, P. *J. Phys. Chem.* **1970**, *74*, 1466.